Chapter 16
Neolithic Transitions: Diffusion of People or Diffusion of Culture?

Joaquim Fort

16.1 Introduction

The Neolithic transition is defined as the shift from hunting-gathering (Mesolithic) into farming and stockbreeding (Neolithic). When did it happen? In Archeology, years Before Present (BP) are defined as years before 1950 AD. The Neolithic arrived from the Near East into Southeastern Europe at about 8000 years BP. Then it spread gradually westwards and northwards, until about 5000 yr BP (Fig. 16.1). Europe is the continent for which more Neolithic sites per unit area have been dated. This is the reason why most models on Neolithic transitions were originally applied to Europe. The spread of farming in Europe can be seen in Fig. 16.1, which is an spatial interpolation of the dates of 918 early Neolithic sites [1] based on a database gathered by archeologist M. vander Linden [2].

As pointed out by Lemmen and Gronenborn (Chap. 17, this volume), it is always important to attempt higher levels of data density and quality. However, the arrival times of the Neolithic at several areas (e.g., Greece, southern Italy, Germany, and England) are similar in Figs. 16.1 and 17.1. Note that Fig. 16.1 uses years BP. In contrast, Fig. 17.1 uses years before Christ (BC).

In this chapter, our first aim is to use an interpolation map (Fig. 16.1) to obtain a mathematically justified map of local speeds of the Neolithic front (this is not possible using drawings such as Fig. 17.1). Once we have a speed map, we will

The original version of this chapter was previously published non-open access. A Correction to this chapter is available at https://doi.org/10.1007/978-3-031-05946-9_24

J. Fort (✉)
Complex Systems Laboratory and Physics Department, Universitat de Girona, C/Ma. Aurèlia Capmany 61, 17071 Girona, Catalonia, Spain
e-mail: joaquim.fort@udg.edu

Catalan Institution for Research and Advanced Studies (ICREA), Passeig Lluís Companys 23, 08010 Barcelona, Catalonia, Spain

© The Author(s) 2023, corrected publication 2024

A. Bunde et al. (eds.), *Diffusive Spreading in Nature, Technology and Society*,
https://doi.org/10.1007/978-3-031-05946-9_16

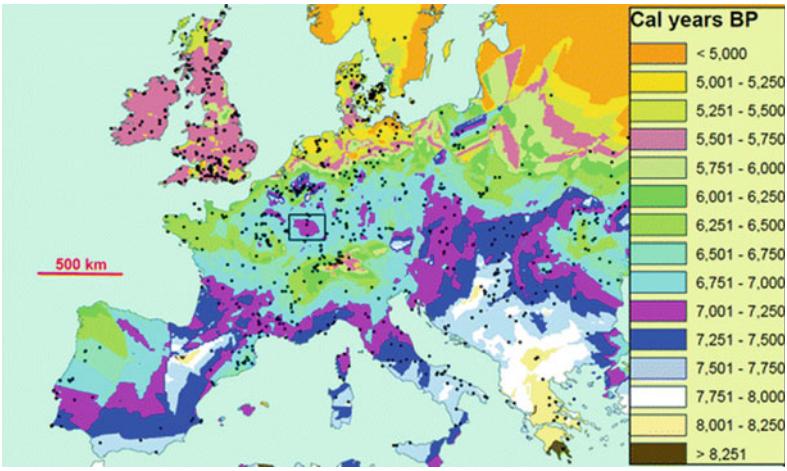

Fig. 16.1 Interpolation of the dates of 918 early Neolithic sites (circles). Each color corresponds to a 250-year interval. We see that the oldest sites are located in the southeast. Note also that farming propagated faster westwards than northwards. Moreover, slowdowns in the Alps and Northern continental Europe are clearly displayed. The patch inside the black rectangle is an example of an anomalously old region, as compared to its surroundings. Due to the paucity of sites, the contours are less detailed in some regions (e.g., upper right and lower left). This map was obtained by means of universal linear kriging interpolation. Dates are given in calibrated years Before Present (BP), as defined in the main text (calibration is a well-known correction, due to the fact that the percentage of radioactive carbon in the atmosphere is not constant). Adapted from Ref. [1]

explore possible explanations in terms of human behavior by making use of the appropriate generalized diffusion equations.

Figure 16.1 shows at once that we are dealing with a gradual spread. Of course, there are some anomalously old/young regions (e.g., the patch inside the black rectangle in Fig. 16.1). Different interpolation methods yield some differences for small anomalous regions, but those of the size of that inside the rectangle in Fig. 16.1 and larger usually appear independently of the interpolation method used. The existence of rivers, mountains, different types of soils, etc., probably makes some areas more attractive for farmers than others. This is one of the reasons why the presence of anomalously old or young regions in interpolation maps is probably unavoidable (even if we had a database totally free of errors and with all dates corresponding exactly to the earliest farming activity at each site). A very clear example are the Alps. These mountains cause an anomalously young region (as compared to its surroundings) in Fig. 16.1. This Alpine region contains many sites and is anomalously young, independently of the interpolation method and also of the database used. Thus anomalous regions are not necessarily artifacts arising from limitations of the database and/or the interpolation technique. Nevertheless, some of them may certainly be artifacts, especially if they contain few or no sites and their presence depends on the interpolation method and/or database used. This is probably the case for the anomalously old region inside the rectangle in Fig. 16.1. It is possible that

using future databases this region will not appear (e.g., because a site inside it is erroneously too old and/or some sites at the right of it are erroneously too early). However, practice in spatial interpolation of Neolithic dates shows that some such anomalous regions always appear (and usually we have no means to know their origin). But this should not be a problem after all. Smoothing techniques are well-established in geographic analysis. They yield, with increasing coarse graining, maps with decreasing subtleness, where sufficiently small anomalous regions gradually disappear without substantially modifying the overall spread pattern. For example, Fig. 16.2b has been obtained from Fig. 16.1 by applying 10 times a smoothing procedure that simply replaces the date of each spatial point in the interpolation grid by the average of that date and those of the 8 surrounding points. It is seen that the isochrones in Fig. 16.2b are smoother than those in Fig. 16.1. By repeating this smoothing procedure more times, we obtain still smoother isochrones (Fig. 16.2c). This makes it possible to analyze the overall spatial trends by getting rid of irrelevant local features that are likely artifacts due to our limited knowledge (not all sites have been discovered, and sources of error exist). For example, the anomalously old region in the rectangle in Fig. 16.1 has disappeared in Fig. 16.2c but the continental trend in the dates (i.e., the gradual decrease westwards and northwards) remains. It is worth to mention that in this way, a totally disordered map of speed vectors becomes a coherent, meaningful directional map of the Neolithic spread (Figs. S1 and 2 in Ref. [1]). For these reasons, smoothing seems a reasonable procedure to estimate local speed directions and magnitudes (in kilometers per year) [1], as we will see below. Note that this is obviously impossible from drawings such as Fig. 17.1. The aim of Chap. 17 is a different one, because it is based on a mathematical model that their authors have compared, similarly to other researchers [3–5], to the average speed implied by the dates obtained by radiocarbon dating (Sect. 17.3 in this volume and Ref. [6]). At the end of this chapter, we will discuss the mathematical model used in Chap. 17.

The spread of the Neolithic in Europe was clearly gradual, because as we move westwards and northwards, we find more and more recent dates (Figs. 16.1 and 17.1). This suggests that it may make sense to apply diffusive models to the spread of the Neolithic. A quantitative justification is the following. We know from Chap. 2 that diffusion equations provide large-scale descriptions of systems where there are, at the small scale, molecules or individuals following random walks (see Fig. 2.5). Does this scenario apply to the spread of the Neolithic? For the moment, assume a very simple model in which agriculture would have spread only due to the dispersal of farmers. Then each random walk is the trajectory obtained by joining, e.g., the birthplaces of an individual's parent, the individual in question, one of his/her children, and so on. Looking at Fig. 16.1, we can easily estimate that agriculture spread from Greece to the Balkans and Central Europe at a speed of roughly 1 km/year. Thus, assuming a generation time of about 32 year [7], farming spread about 32 km per generation. This is much less than the scale of Fig. 16.1 (about 3000 km). This comparison provides a quantitative justification for the use of diffusion-type equations in models of the Neolithic spread.

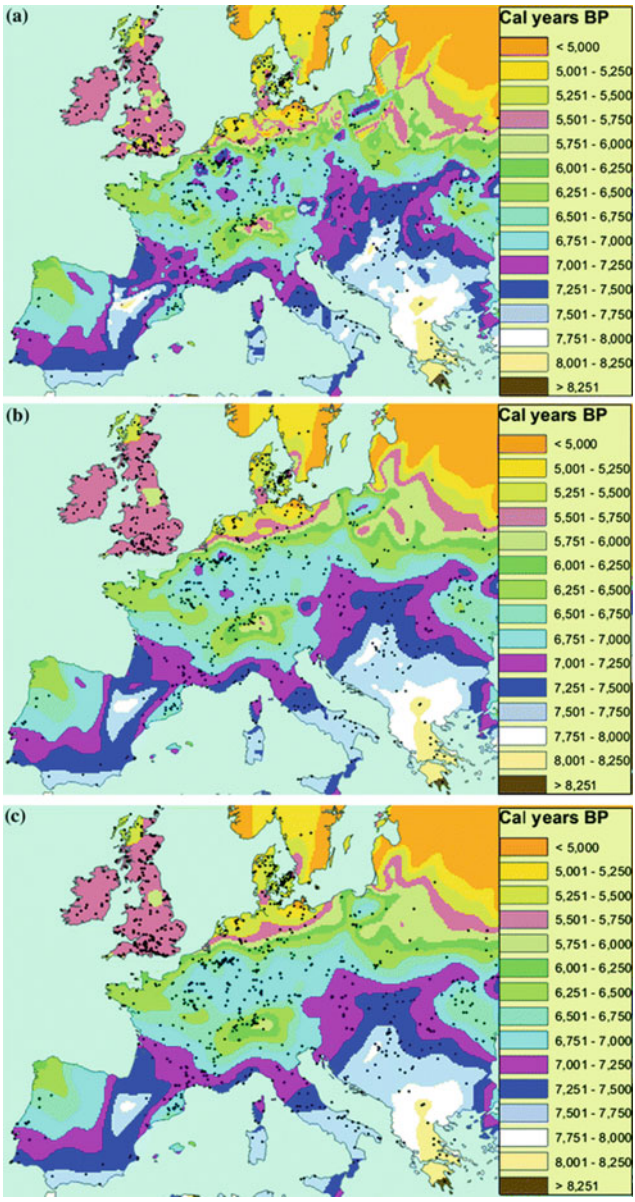

Ammerman and Cavalli-Sforza [8] were the first to apply a diffusive model to the spread of the Neolithic. They used Fisher's wave-of-advance model. In this model, the speed of the Neolithic front is given by Eq. (2.17),

$$v_{Fisher} = 2\sqrt{D\alpha}, \tag{16.1}$$

◀**Fig. 16.2** Isochrones obtained by smoothing ("coarse graining") the map in Fig. 16.1 a single time (**a**), 10 times (**b**) and 20 times (**c**) (i.e. with 1, 10, and 20 iteration steps, where each step consists in replacing the date of each individual point of the map by the average of that date and those of the 8 surrounding points of the square interpolation grid). A map obtained by smoothing 40 times is included as Fig. 16.4a. Note that anomalous regions (such as that inside the black rectangle in Fig. 16.1) gradually disappear. This is useful to perform quantitative estimates of local speed vectors and magnitudes (see Fig. 16.4b for the latter). Adapted from Ref. [1], Supp. Info. Appendix, Sect. S1

where D is the diffusion coefficient and α the initial growth rate (i.e., the net reproduction rate at low population densities). This relation has already been introduced as Eq. (2.17) in Chap. 2. Following Ref. [3] we sketch, for the interested reader, the line of reasoning leading, eventually, to this relation.

Let $N(x, y, t)$ stand for the population density of Neolithic individuals (i.e., farmers), where x and y are Cartesian coordinates and t is the time. We assume that a well-defined time scale T between two successive migrations occurs. This model (to be improved in Sect. 16.3) is based on the assumption (see Ref. [9], Sect. 11.2) that, between the values t and $t + T$, we can add up the changes in the number of individuals in an area differential $ds = dx\,dy$ due to migrations (sub index m) and to population growth (sub index g),

$$[N(x, y, t + T) - N(x, y, t)]ds = [N(x, y, t + T) - N(x, y, t)]_m ds + [N(x, y, t + T) - N(x, y, t)]_g ds. \quad (16.2)$$

Let Δ_x and Δ_y stand for the coordinate variations of a given individual during T. We introduce the dispersal kernel $\phi_N(\Delta_x, \Delta_y)$, defined such that $\phi_N(\Delta_x, \Delta_y)$ is the probability per unit area to move from $(x + \Delta_x, y + \Delta_y)$ at time t to (x, y) at time $t + T$. We can rewrite the parentheses in the first term on the right as

$$[N(x, y, t + T) - N(x, y, t)]_m = \int_{-\infty}^{\infty}\int_{-\infty}^{\infty} N_\Delta \phi_N d\Delta_x d\Delta_y - N(x, y, t) \approx \frac{\langle\Delta^2\rangle}{4}\left(\frac{\partial^2 N}{\partial x^2} + \frac{\partial^2 N}{\partial y^2}\right), \quad (16.3)$$

where N_Δ stands for $N(x + \Delta_x, y + \Delta_y, t)$, and ϕ_N for $\phi_N(\Delta_x, \Delta_y)$. In the last line in Eq. (16.3), we have performed a second-order Taylor expansion in Δ_x and Δ_y, and taken into account that $\int_{-\infty}^{\infty}\int_{-\infty}^{\infty} \phi_N d\Delta_x d\Delta_y = 1$. We have also assumed that the kernel is isotropic, i.e.,

$$\phi_N(\Delta_x, \Delta_y) = \phi_N(-\Delta_x, \Delta_y) = \phi_N(\Delta_x, -\Delta_y), \quad (16.4)$$

and introduced the mean-squared displacement as

$$\left\langle \Delta^2 \right\rangle = \int_{-\infty}^{\infty} \int_{-\infty}^{\infty} \Delta^2 \phi_N(\Delta_x, \Delta_y) d\Delta_x d\Delta_y, \tag{16.5}$$

where $\Delta^2 = \Delta_x^2 + \Delta_y^2$. Note that Eq. (16.4) implies that $\left\langle \Delta_x \right\rangle = 0, \left\langle \Delta_y \right\rangle = 0$, $\left\langle \Delta_x \Delta_y \right\rangle = 0$ and $\left\langle \Delta_x^2 \right\rangle = \left\langle \Delta_y^2 \right\rangle$, which has been applied in the last step in Eq. (16.3). This is Einstein's approach to diffusion [10].

Finally we rewrite the parentheses in the last term in Eq. (16.2) as a Taylor expansion,

$$[N(x, y, t + T) - N(x, y, t)]_g = \left(T F(x, y, t) + \frac{T^2}{2} \frac{\partial F}{\partial t} + \ldots \right) \tag{16.6}$$

where $F(x, y, t)$ is the change in population density per unit time, due to births and deaths.

Expanding the left-hand side of Eq. (16.2) up to first order and collecting terms, we arrive at Fisher's reaction-diffusion equation,

$$\frac{\partial N}{\partial t} = D \left(\frac{\partial^2 N}{\partial x^2} + \frac{\partial^2 N}{\partial y^2} \right) + F(x, y, t), \tag{16.7}$$

where we have introduced the diffusion coefficient,

$$D = \frac{\left\langle \Delta^2 \right\rangle}{4T}. \tag{16.8}$$

which is the two-dimensional analogue of the one-dimensional Eq. (2.3). Concerning the net reproduction function $F(x, y, t)$, in Chap. 2 an example is presented such that

$$F(x, y, t) = \alpha N(x, y, t) \tag{16.9}$$

(see the last term in Eq. (2.15)). This reproduction function corresponds to exponential growth, because without diffusion ($D = 0$) Eq. (16.7) yields $N = N_0 \exp[\alpha t]$, with $N_0 = N(t = 0)$. Thus Eq. (16.9) is an example of interest, but the population density would never stop growing. A biologically more realistic case is the so-called logistic growth function,

$$F(x, y, t) = \alpha N(x, y, t) \left[1 - \frac{N(x, y, t)}{N_{max}} \right], \tag{16.10}$$

where N_{max} is the saturation density, i.e., the population density at which net reproduction vanishes (note that $F(x, y, t) = 0$ if $N(x, y, t) = N_{max}$). The functions of

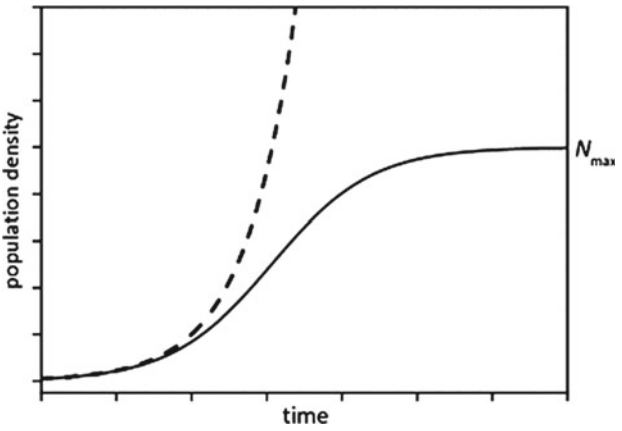

Fig. 16.3 Plots of population density N versus time t. The dashed line corresponds to exponential growth, $N = N_0 e^{\alpha t}$ (see the text below Eq. (16.9)), and the full line to logistic growth, $N = N_0 N_{max} e^{\alpha t}/(N_{max} + N_0(e^{\alpha t} - 1))$ (see Eq. (16.12))

exponential and logistic growth are compared in Fig. 16.3. A more detailed introduction into the formalism of logistic growth is provided by Sect. 3.4.1 of Chap. 3, with an example of the benefit of this reasoning on predicting the spreading of technological innovations given in Sect. 14.2.2 of Chap. 14.

Equation (16.7) with the logistic growth function (16.10) is called Fisher's equation. For our purposes here, we can consider the simple case in which all parameters (D, α and N_{max}) are independent of x, y and t. Travelling wave solutions (also called fronts or waves of advance) are defined as constant-shape solutions, i.e., those depending not on x, y and t separately but only on $z = r - vt$, where v is the front speed and $r = \sqrt{x^2 + y^2}$ the radial coordinate.

Kolmogorov et al. [11] showed that in Fisher's model, a front is formed and its speed is given by Eq. (16.1), assuming that initially the population density $N(x, y, t)$ has compact support. In practice, this assumption means that $N(x, y, t = 0) = 0$ everywhere except in a finite region. This is biologically realistic, in contrast to solutions such that $N(x, y, t = 0) \neq 0$ for all values of x, y ($-\infty < x < \infty$, $-\infty < y < \infty$). The latter solutions are not biologically realistic, because in practical applications we always want to analyze the spread of organisms that are initially present in a finite region of space.

Using variational methods, Aronson and Weinberger [12] also showed that the speed of front solutions to Fisher's equation is given by Eq. (16.1) (see Sect. IV.A in Ref. [13] for a simple derivation based on variational principles).

Importantly, Fisher's wave-of-advance speed (1) does not depend on N_{max}. Moreover, this speed is the same as for exponential growth (Eq. (16.9)), see Eq. (2.17). Thus, the wave-of-advance speed is the same in both the logistic and the exponential models. However, their shape is different, because for exponential growth the population density keeps growing in time, whereas for logistic growth it stops growing at

$N = N_{max}$ (see Fig. 16.3). Thus, the waves of advance under logistic growth have the profile shown in Fig. 2.6, where we can see that the population density stops growing once $N = N_{max}$. In contrast, for exponential growth, the population density keeps growing forever everywhere (see Ref. [14], Figs. 3.3 and 3.6).

Returning to the spread of the farming, Ammerman and Cavalli-Sforza [8] noted from archeological dates that the speed of the Neolithic wave of advance was about 1 km/year. They next asked the following interesting question: what speed does Fisher's model (Eq. (16.1)) predict? In order to answer this, empirical values for $\langle \Delta^2 \rangle$ and T are needed to estimate D using Eq. (16.8). Additionally, an empirical value for α is needed to estimate the speed from Eq. (16.1). Ethnographic observations of preindustrial populations have measured the displacement of individuals and found the average for the mean-squared displacement per generation $\langle \Delta^2 \rangle = 1288$ km^2 [1, 15] and the mean generation time (defined as the age difference between a parent and his/her children) $T = 32$ year [7]. Thus, we obtain from Eq. (16.8) $D = 10$ km^2/year. On the other hand, for populations which settle in empty space, $N \ll N_{max}$ and Eq. (16.10) reduces to (16.9), so that we can fit exponential curves (graphically, we can understand this because both curves in Fig. 16.3 overlap in the left-hand side). Ethnographic data yield the average exponent $\alpha = 0.028$ year^{-1} [15]. Using these values in Eq. (16.1), we estimate a front speed of about 1 km/year, which is similar to the speed obtained from the archeological observations. Indeed, as mentioned above, looking at Fig. 16.1, we can easily estimate that agriculture spread from Greece to the Balkans and Central Europe at a speed of roughly 1 km/year (more precise estimations with recent data, based on regression analysis [4] and geostatistical techniques [1], agree with this average). This agreement was first noted by Ammerman and Cavalli-Sforza [5, 8]. In this way, Ammerman and Cavalli-Sforza noted that diffusive models are useful not only because they make it possible to describe mathematically a major event in prehistory (the spread of agriculture), but also because they indicate a possible mechanism for it, namely the spread of people (i.e., of populations of farmers). They called this demic diffusion (from the Greek word *demos*, which means people). In contrast, most authors at the time advocated for the learning of farming by hunter-gatherers (i.e., for the spread of agriculture without substantial spread of people) [16]. The latter mechanism is called cultural diffusion.

16.2 First Improvement: Beyond the Second-Order Approximation

In the derivation of Eq. (16.7) we have performed Taylor expansions up to first order in time and second order in space. Without those approximations we obtain, instead of Eq. (16.7),

$$N(x, y, t+T) - N(x, y, t) = \int_{-\infty}^{\infty}\int_{-\infty}^{\infty} N_{\Delta}\phi_N d\Delta_x d\Delta_y - N(x, y, t) + R_T[N(x, y, t)]), \tag{16.11}$$

where the joint effects of reproduction and survival are, again, well-described by the solution to a logistic growth function, namely [9]

$$R_T[N(x, y, t)] = \frac{e^{\alpha T} N_{max} N(x, y, t)}{N_{max} + (e^{\alpha T} - 1)N(x, y, t)}. \tag{16.12}$$

When observed dispersal data are used, the kernel *per unit length* $\varphi_N(\Delta)$ is defined as the probability to disperse into a ring of radius Δ and width $d\Delta$, divided by $d\Delta$. If individuals of the population N have probabilities p_j to disperse at distances r_j ($j = 1, 2, \ldots, M$), we can write

$$\varphi_N(\Delta) = \sum_{j=1}^{M} p_j \delta^{(1)}(r_j), \tag{16.13}$$

where $\delta^{(1)}(r_j)$ is the 1D Dirac delta centered at r_j (i.e., a function that vanishes everywhere except at $\Delta = r_j$). Since the total probability must be one,

$$1 = \int_0^{\infty} \varphi_N(\Delta) d\Delta, \tag{16.14}$$

and $\varphi_N(\Delta)$ is clearly a probability *per unit length*. In contrast, the kernel $\phi_N(\Delta_x, \Delta_y)$ in Eq. (16.11) is a probability *per unit area* (because it is multiplied by $d\Delta_x d\Delta_y$, which has units of area). The normalization condition for $\phi_N(\Delta_x, \Delta_y)$ is therefore

$$1 = \int_{-\infty}^{\infty}\int_{-\infty}^{\infty} \phi_N(\Delta_x, \Delta_y) d\Delta_x d\Delta_y = 2\pi \int_0^{\infty} \phi_N(\Delta) \Delta d\Delta, \tag{16.15}$$

where we have used polar coordinates $\Delta = \sqrt{\Delta_x^2 + \Delta_y^2}$, $\theta = tan^{-1}\frac{\Delta_y}{\Delta_x}$ and assumed the kernel is isotropic, $\phi_N(\Delta_x, \Delta_y) = \phi_N(\Delta)$. Comparing Eqs. (16.14) and (16.15), we see that the dispersal probability per unit length (i.e., into a ring of area $2\pi\Delta d\Delta$) $\varphi_N(\Delta)$ is related to that per unit area $\phi_N(\Delta)$ as [17]

$$\varphi_N(\Delta) = 2\pi\Delta\phi_N(\Delta) \tag{16.16}$$

and Eq. (16.13) yields

$$\phi_N(\Delta) = \sum_{j=1}^{M} p_j \frac{\delta^{(1)}(r_j)}{2\pi\Delta}. \tag{16.17}$$

For homogeneous parameter values, the speed will not depend on direction and can thus be more easily computed along the x-axis ($y = 0$). Consider a coordinate frame $z = x - vt$ moving with the wave of advance (v is the front speed). The population density of farmers will be equal to its saturation density in regions where the Neolithic transition is over, and it will decay to zero in regions where few farmers have arrived. Thus, we assume as usual the *ansatz* [17] $N(x, y, t) \approx N_0 \exp[-\lambda z] \to 0$ for $z \to \infty$ (with $\lambda > 0$). Then, assuming that the minimum speed is that of the front (which has been verified by numerical simulations), we obtain for the speed v of front solutions to Eq. (16.11) [15]

$$v_{NCohab} = \min_{\lambda>0} \frac{\ln\left[(e^{\alpha T} - 1)\sum_{j=1}^{M} p_j I_0(\lambda r_j)\right]}{T\lambda}, \tag{16.18}$$

where the sub index $NCohab$ indicates that this is *not* a cohabitation model (see the next section), and $I_0(\lambda r_j)$ is the modified Bessel function of the first kind and order zero. In this model, the speed can be found by plotting the fraction in Eq. (16.18) as a function of λ and finding its minimum.

In Ref. [15], it has been shown that the differences in the front speed obtained from Eq. (16.13) and Fisher's approximation, Eq. (16.1), are up to 49% for human populations. So the effect of higher-order terms is not negligible.

16.3 Second Improvement: Cohabitation Equations

For human populations, newborn children cannot survive on their own. However, when they come on age they can move away from their parents. This point has led some authors to use an equation of the so-called cohabitation type, namely

$$N(x, y, t + T) = \int_{-\infty}^{\infty}\int_{-\infty}^{\infty} R_T[N_\Delta]\phi_N d\Delta_x d\Delta_y, \tag{16.19}$$

where $R_T[N]$ is again given by Eq. (16.12). Then the speed of front solutions is [15, 18]

$$v_{Cohab} = \min_{\lambda>0} \frac{\alpha T + \ln\left[\sum_{j=1}^{M} p_j I_0(\lambda r_j)\right]}{T\lambda}. \tag{16.20}$$

The reason why Eq. (16.19) is more reasonable than Eq. (16.11) is that, clearly, Eq. (16.11) assumes that individuals born at (x, y) at time t (last-but-one term) will not move at all, i.e., they will all still be at (x, y) on coming of age (time $t + T$, left-hand side). Thus, for example, in the simple case in which all parents move, they will leave all of their children alone. Such an anthropologically unrealistic feature makes it clear that Eq. (16.11) is less accurate than Eq. (16.19). For additional derivations and figures showing that Eq. (16.11) is less realistic than the cohabitation Eq. (16.19), see especially Fig. 1 in Ref. [15], Fig. 17 in Ref. [17], and Ref. [18].

A more direct way to see the limitations of Fisher's speed (16.1) is to note that it yields $v_{Fisher} \to \infty$ for $\alpha \to \infty$. In contrast, it has been shown that the cohabitation speed (16.20) yields for $\alpha \to \infty$ the value $v_{Cohab} = r_{max}/T$, i.e., the maximum dispersal distance divided by the generation time (see Fig. 2 in Ref. [15]), which is physically reasonable. Moreover, the error of Fisher's speed (16.1) relative to Eq. (16.20) reaches 30% for realistic human kernels and parameter values [15]. This error is still larger when cultural diffusion is included [1] (next section).

16.4 Demic-Cultural Model

Up to now we have only considered equations with a single mechanism for the spread of the Neolithic, namely the dispersal of farmers (demic diffusion). But agriculture can be also learnt by hunter-gatherers (cultural diffusion). When this conversion of hunter-gatherers into farmers (cultural transmission) is taken into account, we might be tempted to generalize Eq. (16.19) into

$$N(x, y, t + T) = \int_{-\infty}^{\infty}\int_{-\infty}^{\infty} R_T[N_\Delta]\phi_N d\Delta_x d\Delta_y + \int_{-\infty}^{\infty}\int_{-\infty}^{\infty} c[N_\Delta, P_\Delta]\phi_N^{converts} d\Delta_x d\Delta_y, \tag{16.21}$$

where $P_\Delta = P(x + \Delta_x, y + \Delta_y)$ is the population density of hunter-gatherers at $(x + \Delta_x, y + \Delta_y)$. The cultural transmission function $c[\ldots]$ in Eq. (16.21) is due to the conversion of hunter-gatherers into farmers. Thus, a similar equation for the population density of hunter-gatherers $P\ (x, y, t + T)$ could be proposed, with a minus sign in the last term. A recent derivation has found for the cultural transmission function $c[\ldots]$ (see Ref. [19], Eq. (1))

$$c[N(x, y, t), P(x, y, t)] = f\frac{N(x, y, t)P(x, y, t)}{N(x, y, t) + \gamma P(x, y, t)}, \tag{16.22}$$

where f and γ are cultural transmission parameters. The kernel $\phi_N^{converts}(\Delta_x, \Delta_y)$ in Eq. (16.22) is the dispersal kernel of hunter-gatherers that have been converted into farmers. Since they now behave as farmers, let us assume that this kernel is the same as $\phi_N(\Delta_x, \Delta_y)$. Then Eq. (16.22) becomes

$$N(x, y, t+T) = \int_{-\infty}^{\infty}\int_{-\infty}^{\infty} R_T[N_\Delta]\phi_N d\Delta_x d\Delta_y + \int_{-\infty}^{\infty}\int_{-\infty}^{\infty} f\frac{N_\Delta P_\Delta}{N_\Delta + \gamma P_\Delta}\phi_N d\Delta_x d\Delta_y. \tag{16.23}$$

A model of this kind was applied recently (see Eq. 5 in Ref. [19]). It is an approximation that may be valid in some regions (with mainly demic diffusion) but it cannot lead to a purely cultural model of Neolithic spread (because according to Eq. (16.23) there is no front propagation in the absence of demic diffusion, i.e., if $\phi_N(\Delta_x, \Delta_y) \neq 0$ only at vanishing distance, i.e., for $\Delta = (\Delta_x^2 + \Delta_y^2)^{1/2} = 0$). Thus we will here consider a more realistic model in two ways. Firstly we take into account that, according to ethnographic observations, hunter-gatherers can learn agriculture from farmers located some distance away [1]. Then Eq. (16.23) is generalized into

$$\begin{aligned} N(x, y, t+T) = &\int_{-\infty}^{\infty}\int_{-\infty}^{\infty} R_T[N_\Delta]\phi_N d\Delta_x d\Delta_y \\ &+ \int_{-\infty}^{\infty}\int_{-\infty}^{\infty} \phi_N d\Delta_x d\Delta_y \int_{-\infty}^{\infty}\int_{-\infty}^{\infty} \phi_P' d\Delta_x' d\Delta_y' f\frac{N_{\Delta+\Delta'} P_\Delta}{N_{\Delta+\Delta'} + \gamma P_\Delta}, \end{aligned} \tag{16.24}$$

where $N_{\Delta+\Delta'}$ stands for $N(x + \Delta_x + \Delta_x', y + \Delta_y + \Delta_y', t)$.

In practice, the cultural kernel $\phi_P'(\Delta_x', \Delta_y')$ (which is abbreviated as ϕ_P' in Eq. (16.24)) is a set of probabilities P_k for hunter-gatherers to learn agriculture from farmers living at distances $R_k = (\Delta_x'^2 + \Delta_y'^2)^{1/2}$, during a generation time T. This is similar to the fact, mentioned above Eq. (16.13), that in practice the demic kernel $\phi_N(\Delta_x, \Delta_y)$ is a set of probabilities p_j for farmers to disperse at distances $r_j = (\Delta_x^2 + \Delta_y^2)^{1/2}$, also during a generation time T.

Secondly, we note that after a generation time T, reproduction will have led to new individuals not only in the population of farmers (first line in Eq. (16.24)) but also in the population of hunter-gatherers converted into farmers (second line in Eq. (16.24)). Thus we finally generalize Eq. (16.24) into

$$N(x, y, t+T) = \int_{-\infty}^{\infty}\int_{-\infty}^{\infty} R_T[N_\Delta]\phi_N d\Delta_x d\Delta_y$$

$$+\int_{-\infty}^{\infty}\int_{-\infty}^{\infty}\phi_N d\Delta_x d\Delta_y \int_{-\infty}^{\infty}\int_{-\infty}^{\infty}\phi_P' \, d\Delta_x' d\Delta_y' R_T \left[f \frac{N_{\Delta+\Delta'} P_\Delta}{N_{\Delta+\Delta'} + \gamma P_\Delta} \right]. \tag{16.25}$$

The speed of front solutions to Eq. (16.25) is [1]

$$v = \min_{\lambda>0} \frac{\alpha T + \ln\left[\left(\sum_{j=1}^{M} p_j I_0(\lambda r_j)\right)\left(1 + C\left[\sum_{k=1}^{Q} P_k I_0(\lambda R_k)\right]\right)\right]}{T\lambda}, \tag{16.26}$$

with $C = f/\gamma$. This reduced parameter C was called the intensity of cultural transmission [19] because, according to Eq. (16.22), $C = f/\gamma$ is the number of hunter-gatherers converted per farmer at the front leading edge (i.e., in regions such that $N \ll P$). Without cultural transmission ($C = 0$), the demic-cultural front speed, given by Eq. (16.26), reduces to the purely demic speed, Eq. (16.20), as it should. With frequency-dependent cultural transmission, Eq. (16.22) is more complicated and the equations are longer, but the final results are exactly the same [1].

It is important to note that cultural transmission (the factor in brackets $[f \ldots]$ at the end of the second line in Eq. (16.25)) is applied in a term that also contains the effects of net reproduction (R_T) and dispersal (the kernel of farmers $\phi_N(\Delta_x, \Delta_y)$). Thus, some hunter-gatherers will learn agriculture from farmers located a distance (Δ_x', Δ_y'), and the children of those converted hunter-gatherers will possibly move a distance (Δ_x, Δ_y) (similarly to the children of farmers, first line). Therefore, some hunter-gatherers can learn agriculture from farmers and the next generation (i.e., the children) of those hunter-gatherers will be farmers, in agreement with ethnographic data [20].

Finally, a purely cultural model means no demic diffusion. In this model, the front speed can be obtained from Eq. (16.26) without demic diffusion ($r_1 = 0$ and $p_1 = 1$), namely

$$v_C = \min_{\lambda>0} \frac{\alpha T + \ln\left[1 + C\left(\sum_{k=1}^{Q} P_k I_0(\lambda R_k)\right)\right]}{T\lambda}, \tag{16.27}$$

where the sub index C stands for purely cultural diffusion. This is the purely cultural analogue to the purely demic speed given by Eq. (16.20). Both of them are, of course, cohabitation models.

16.5 Demic Versus Cultural Diffusion in the Spread of the Neolithic in Europe

What do the models above imply for the relative importance of demic and cultural diffusion in the spread of the Neolithic in different regions of Europe? Let us first

summarize a proposal [1], and later we will discuss an alternative possibility. First of all, we need ranges for the parameters appearing in our equations.

The ranges for α and T that have been measured for preindustrial farming populations are $0.023\,\text{year}^{-1} \leq \alpha \leq 0.033\,\text{year}^{-1}$ and $29\,\text{year} \leq T \leq 35\,\text{year}$ (see the *SI Appendix* to Ref. [19] for details).

The dispersal kernel $\phi_N(\Delta_x, \Delta_y)$ has been measured for each of the following five preindustrial farming populations [15]. For each population, we give its purely demic speed range, as predicted by the cohabitation model, Eq. (16.20), with its dispersal kernel as well as $\alpha = 0.023\,\text{year}^{-1}$ and $T = 35\,\text{year}$ (slowest speed) or $\alpha = 0.033\,\text{year}^{-1}$ and $T = 29\,\text{year}$ (fastest speed).

- Population A (Gilishi 15): purely demic speed range 0.87–1.15 km/year.
- Population B (Gilishi 25): purely demic speed range 0.92–1.21 km/year.
- Population C (Shiri 15): purely demic speed range 1.14–1.48 km/year.
- Population D (Yanomamö): purely demic speed range 1.12–1.48 km/year.
- Population E (Issongos): purely demic speed range 0.68–0.92 km/year.

We see that demic diffusion predicts Neolithic front speeds of at least 0.68 km/year. Demic-cultural diffusion will be still faster. Thus, it has been suggested that perhaps cultural diffusion could be responsible for the Neolithic spread in regions with speeds below 0.68 km/year [1]. For simplicity, let us consider purely cultural diffusion, Eq. (16.27), although a short-range demic kernel can be also included (Sect. S6 in Ref. [1]). In order to estimate the speeds predicted by purely cultural diffusion, we need the following cultural parameters.

The cultural transmission intensity C from hunter-gathering to farming has been estimated from several case studies in Ref. [19] and the overall range is $1.0 \leq C \leq 10.9$.

The cultural kernel has been estimated for each of the following five populations, from distances from hunter-gatherers camp locations to the villages of farmers, where the hunter-gatherers practice agriculture [1]. For each population, we report the purely cultural speed range obtained from Eq. (16.27) using its cultural kernel as well as $\alpha = 0.023\,\text{year}^{-1}$, $T = 35\,\text{year}$ and $C = 1$ (slowest speed) or $\alpha = 0.033\,\text{year}^{-1}$, $T = 29\,\text{year}$ and $C = 10.9$ (fastest speed).

- Population 1 (Mbuti, band I): speed range 0.17–0.36 km/year.
- Population 2 (Mbuti, band II): speed range 0.30–0.57 km/year.
- Population 3 (Mbuti, band III): speed range 0.32–0.66 km/year.
- Population 4 (Aka): speed range 0.09–0.19 km/year.
- Population 5 (Baka): speed range 0.03–0.07 km/year.

Thus, the purely cultural model yields 0.03–0.66 km/year. Note that this is slower than the purely demic speed range found above (0.68–0.92 km/year).

Finally, for the demic-cultural model, Eq. (16.26), the slowest speed is obviously 0.68 km/year (see the purely demic model above). The fastest speed corresponds to the strongest value observed for the intensity of cultural transmission ($C = 10.9$), the fastest cultural kernel (population 3), the fastest demic kernel (population C or D), the highest observed value of α ($0.033\,\text{year}^{-1}$), and the lowest observed value of

T (29 year). Using these data in Eq. (16.25), we find that the fastest speed is obtained for the demic kernel of population D yielding 3.04 km/year.

In Fig. 16.4b, the color scale has been chosen so that the red color corresponds to the regions that can be explained by purely cultural diffusion (0.03–0.66 km/year, from the purely cultural model above). The demic and demic-cultural models predict speeds above 0.68 km/year and are thus too fast to be consistent with the archeological data in the red regions in Fig. 16.4b. This suggests that cultural diffusion could explain the Neolithic transition in Northern Europe, as well as in the Alps and west of the Black Sea. The analysis of the areas where demic diffusion played a role is less straightforward, but it is possible to determine the regions where the speed was *mainly* demic (i.e., where the cultural effect was $< 50\%$) [1]. They correspond to the yellow regions in Fig. 16.4b. The regions where either demic or cultural diffusion could have dominated are the blue regions in Fig. 16.4b. The blue regions appear because we have used parameter ranges and several kernels (they would not appear if we had used a single value for each parameter, a single demic kernel, and a single cultural kernel). Finally, in the green regions in Fig. 16.4, the speed is too fast to agree with any of the three models in the present chapter, but in continental Europe, those regions contain very few sites and will probably disappear using more complete databases (i.e., with more archeological sites).

In order to discuss an alternative possibility, let us note that the models presented in this paper are simple in the sense that there are few parameters but, in spite of this, their estimation is remarkably difficult. Indeed, so far it has not been possible to estimate dispersal kernels, cultural kernels, or cultural transmission intensities from purely archeological data. Therefore, for the time being, the only possibility is to use ethnographic data instead (as already done by Ammerman and Cavalli-Sforza [5] for the parameters in Fisher's model). As long as it is not possible to overcome this limitation, an open possibility will always be that prehistoric parameter values might have been substantially different than those estimated from present preindustrial populations. Recently, archeological data have been used to perform a rough estimation of the growth rate α in Scandinavia, and it leads to a mainly demic spread in spite of the front speed being slow (0.44-0.66 km/year) [21]. This opens a very interesting possibility: if in the future it were possible to estimate growth rates from archeological data for different regions of Europe, the map in Fig. 16.4b could be refined by using a space-dependent growth rate. Thus, if the growth rate α were smaller in northern Europe (as it seems to be in Scandinavia), it is possible that some of the slow regions could be perhaps explained by a mainly demic model (i.e., some of the red regions in Fig. 16.4b could perhaps not be purely cultural). Unfortunately such a study has not been performed yet, because the estimation of regional Neolithic growth rates from archeological data is still in its infancy. But this could be an interesting topic of future research.

In recent years, speeds of Neolithic fronts have been measured in continents other than Europe. This work has led to the proposal of the following general laws of Neolithic spread [22, 23].

1. First law. The Neolithic spreads inland at a rate of about 1 km/year, although there is substantial variation (0.44-3.6 km/year). This law is satisfied in at least the following 13 case studies. It clearly holds for the Neolithic in overall Europe [5, 4], southern Asia [24], the Balkans [25, 26], 3 European ceramic culture areas (namely the Eastern Linear Pottery [25], the LinearBandKeramik [25] and the Trichterbeckerkultur [25]) as well as for the eastern Bantu expansion in Africa [27], the spread of domesticated rice in China and southeastern Asia [28], and the Saladoid-Barrancoid and Incised-Punctuate expansions in tropical South America [29]. In my view, the spread of the Neolithic in Scandinavia [21], the southern Bantu spread, and the expansion of Khoi-khoi herders also support this law, because there is no inconsistency with the facts that (i) the last two case studies also agree with the second law below, and (ii) the Scandinavian one supports the fifth law below.
2. Second law. If in addition to demic diffusion there is substantial cultural diffusion, the Neolithic spreads more rapidly. This law has strong support from mathematical models (Sect. 16.4) and it is consistent with the observed rates for two expansions in which cultural diffusion has been proposed to be of importance, namely those of Khoi-khoi herders in southern Africa [30] and the southern Bantu spread in East Africa [27]. For both case studies (Khoi-khoi and southern Bantu), the lower bounds (1.2 km/year and 1.3 km/year, respectively) are close to 1 km/year, so they also agree with the first law.
3. Third law. Neolithic spread rates over the sea take place at about 10 km/year. Such very fast speeds have been observed in the spread of the Neolithic in the western Mediterranean [31] and Austronesia [32]. More case studies are necessary to determine a range of speeds for Neolithic rates when sea travel is involved. For example, in the eastern Mediterranean the Neolithic spread rate has apparently never been quantified by linear regression.
4. Fourth law. Most inland and coastal Neolithic spreads are mainly demic. The only examples known up to now that might be perhaps mainly cultural are the spread of maize in America [33] and the expansion of Khoi-khoi herders in southern Africa [30]. Anyway, the fourth law is valid for all 13 case studies of farmers listed in the first law, as well as for the coastal spread of the Neolithic along the western Mediterranean [31].
5. Fifth law. The Neolithic tends to spread more slowly at higher latitudes. This law is supported by a well-known slowdown in northern continental Europe (Fig. 16.4b) and, as mentioned above, by a study on the spread of the Neolithic in Scandinavia. In the latter case, it has been noted that the slowness may be due to a small value of the growth rate α, which was estimated directly from archeological data [21]. A low growth rate is perhaps not very surprising, given the fact that in modern human populations reproduction is also known to decrease with increasing latitude [34]. However, it is not yet established by archeological data if the slowness at higher latitudes is (always) due to reduced values of the growth rate or not, so the statement above of the fifth law does not include any explanation for the slowness. The upper bound for the spread rate in Scandinavia

(0.84 km/year) is close to 1 km/year, so this case study also agrees with the first law.

6. Sixth law. The Neolithic spreads later and more slowly at higher altitudes above sea level (compared to surrounding regions). This is clearly suggested by the following results. An interpolation has shown that the Neolithic first surrounded the Alps completely and only later began to climb up these mountains (Fig. 16.1). It did so from all directions (Fig. 2 in Ref. 1) and at clearly slower speeds (Figs. 16.1 and 16.4b).

16.6 Conclusions

The models reviewed in this chapter suggest that the spread of the Neolithic in Europe was (i) fast and mainly demic in the Balkans and Central Europe; (ii) slow and perhaps mainly cultural in Northern Europe, the Alpine region, and west of the Black Sea (Fig. 16.4b) [1]. As seen in Fig. 16.4b, the process was fast (speeds above 0.68 km/year) in Greece, Italy, the Balkans, Hungary, Slovakia, Czechia, and central Germany. This wide region includes a substantial part of the Linearbandkermic (LBK) culture in Central Europe. This is in agreement with the fact that the LBK is widely regarded as demic by archeologists. Also in agreement with our results, some archeologists have argued for the importance of demic diffusion in the Neolithic spread from the Aegean northwards and across the Balkans. On the other hand, in Northern Europe, the Alps, and West of the Black Sea (red color in Fig. 16.4b), the transition was slow (speeds below 0.66 km/year) and, according to our models, possibly not driven by demic neither demic-cultural diffusion. Some archeologists have previously suggested that cultural diffusion had a strong role in the spread of the Neolithic in Northern Europe, the Alps, and West of the Black sea. Note that these are the possibly cultural diffusion regions according to our models (red color in Fig. 16.4b). For detailed archeological references on the importance of demic and cultural diffusion in different regions of Europe, see, e.g., Sect. 3 in Ref. [1]. Ancient genetics also indicates that cultural diffusion was more important in Northern Europe [35]. But it is worth to note that those ancient genetic data were obtained in Latvia and Ukraine, outside Fig. 16.4. Moreover, we have stressed that non-homogeneous reproduction (still to be confirmed or refused using archeological data) could provide an alternative (mainly demic) explanation for the slow areas (red color in Fig. 16.4b).

The slowness of cultural diffusion (as compared to demic diffusion) is due to the fact that, according to ethnographic observations, the distances appearing in the cultural kernel $\phi_P'(\Delta_x', \Delta_y')$ are substantially shorter than those appearing in the demic kernel $\phi_N(\Delta_x, \Delta_y)$ [1]. The intuitive reason may be that agriculture is a difficult cultural trait to learn, and this leads to shorter cultural than demic diffusion distances. Note that the cultural distances are defined as those separating hunter-gatherers from the farmers who teach them how to farm. Indeed, according to ethnographic data, in

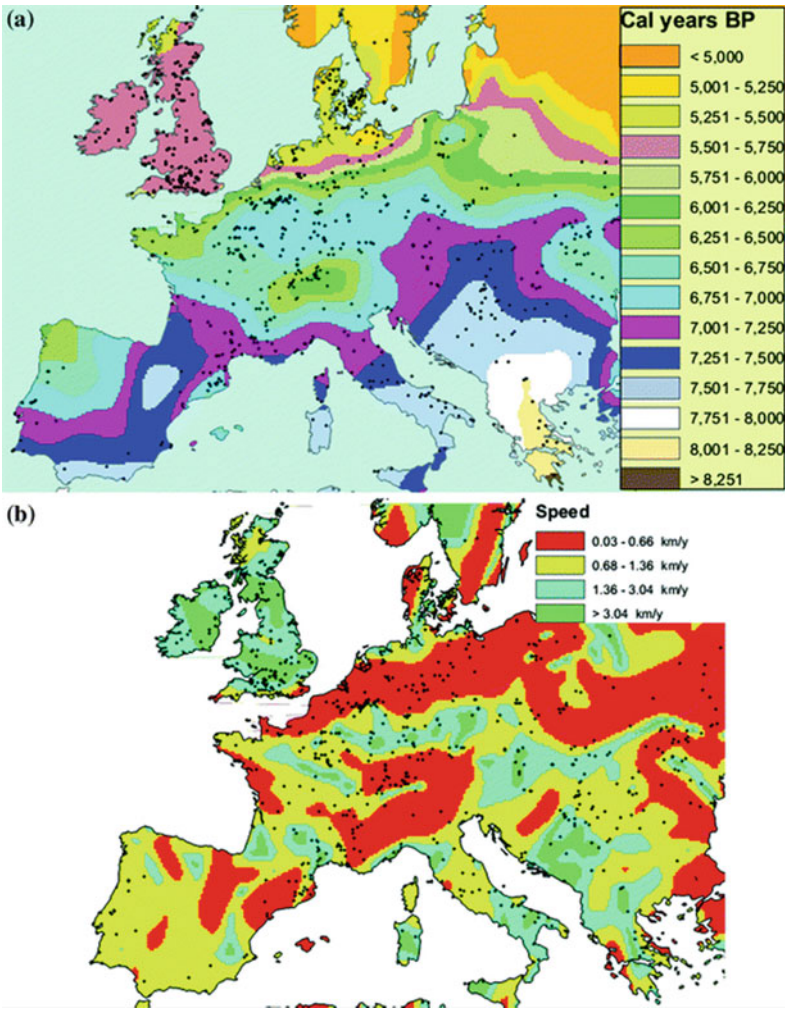

Fig. 16.4 Isochrones obtained by smoothing 40 times the map in Fig. 16.1 (**a**). Note that most anomalously old/recent areas have disappeared. Smoothing 60 times yields almost the same map. **b** Displays the speed ranges obtained from (**a**). Closer isochrones correspond to slower speeds. Adapted from Ref. [1], Supp. Info. Appendix, Fig. S4

the spread of farming cultural diffusion distances were short as compared to demic diffusion distances [1]. The latter are those along which the children of farmers disperse away from their parents. Such demic distances can obviously be larger than cultural distances, because the children of farmers have already learnt agriculture before leaving their parents.

Models similar to those summarized here have been applied to Paleolithic waves of advance [36], language substitution fronts [37], etc.

All models considered in this chapter operate with a minimum of parameters. In the demic model, for instance, the only parameters are the initial growth rate α, the generation T, and the dispersal kernel. Crucially, all three have been estimated from ethnographic or archeological data. With such constraints one is able to largely avoid any unjustified bias in modeling which may easily occur by the use of too many parameters which, finally, degenerate to simple fitting parameters. Using many free parameters, it often turns out that the observed data can be reproduced but the model is based on wrong premises. For example, in some models of virus infection fronts, it was possible to reproduce some experimental front speeds by choosing several parameter values [38, 39]. However, this was not possible for realistic parameter values [39, 40]. Later, different models reproduced the data without choosing any parameter values [41]. Thus, the old models were not appropriate (and missed crucial aspects) because they agree with only some of the data, by using non-realistic equations and parameter values. Again, in the case of Neolithic spread, we have to be aware that one may introduce very large parameter sets as demonstrated in Chap. 17. But there, most of the eight parameter values used are chosen (not derived from independent data) to replicate the observed arrival times of the Neolithic at several regions (this is clearly stated in Ref. [6], p. 3462, and summarized here in Table 17.2 and Fig. 17.6). Thus, their parameter values become questionable with the lack of possibilities for their determination from reliable, independent sources. Besides the parameter values, there are also hypothetical assumptions in some models (e.g., Fig. 17.3). Using as few as possible untested assumptions and unknown parameters in the models often makes them more realistic (we stress that a very clear example is that of virus infection fronts).

Recently, the author has suggested some general laws of Neolithic spread around the world (last part of Sect. 16.5). It is worth to mention that ancient genetic data can be used to constrain better the models by, e.g., estimating the cultural transmission intensity C [42]. In the future, surely many more archeological and genetic data will become available and lead to further conclusions.

References

1. J. Fort, J. R. Soc. Interface **12**, 20150166 (2015)
2. J. Fort, T. Pujol, M. vander Linden, Am. Antiq. **77**, 203 (2012)
3. J. Fort, V. Méndez, Phys. Rev. Lett. **82**, 867 (1999)
4. R. Pinhasi, J. Fort, A.J. Ammerman, PLoS Biol. **3**(e410), 2220 (2005)
5. A.J. Ammerman, L.L. Cavalli-Sforza, *The Neolithic Transition and the Genetics of Populations in Europe* (Princeton University Press, Princeton, 1984)
6. C. Lemmen, D. Gronenborn, K.W. Wirtz, J. Arch. Sci. **38**, 3459 (2011)
7. J. Fort, D. Jana, J.M. Humet, Phys. Rev. E **70**, 031913 (2004)
8. A.J. Ammerman, L.L. Cavalli-Sforza, in *The Explanation of Culture Change: Models in Prehistory*, ed. by C. Renfrew (Duckworth, London, 1973), pp. 343–357
9. J.D. Murray, *Mathematical Biology*, vol. 1 (Springer, Berlin, 2001)
10. A. Einstein, *Investigations on the Theory of Brownian Movement* (Dover, New York, 1956)
11. A.N. Kolmogorov, I.G. Petrovsky, N. Piskunov, Bull. Univ. Moscow Ser. Int. A **1**, 1 (1937)

12. D.G. Aronson, H.F. Weinberger, Adv. Math. **30**, 33 (1978)
13. V. Méndez, J. Fort, J. Farjas, Phys. Rev. E **60**, 5231 (1999) (Sect. IV.A)
14. N. Shigesada, K. Kawasaki, *Biological Invasions: Theory and Practice* (Oxford University Press, Oxford, 1997)
15. N. Isern, J. Fort, J. Pérez-Losada, J. Stat. Mech. **2008**, P10012 (2008)
16. M.S. Edmonson, Curr. Anthropol. **2**, 71 (1961)
17. J. Fort, T. Pujol, Rep. Prog. Phys. **71**, 086001 (2008)
18. J. Fort, J. Pérez-Losada, N. Isern, Phys. Rev. E **76**, 031913 (2007)
19. J. Fort, Proc. Natl. Acad. Sci. U.S.A. **109**, 18669 (2012)
20. J.D. Early, T.N. Headland, *Population Dynamics of a Philippine Rain Forest People. The San Ildefonso Agta* (University Press of Florida, Gainesville, 1998)
21. J. Fort, J.M. Pareta, L. Sorensen, J. R. Soc. Interface **15**, 20180597 (2018)
22. J. Fort, The spread of agriculture: quantitative laws in prehistory?, in *Simulating Transitions to Agriculture in Prehistory*, ed. by S. Pardo-Gordó, S. Bergin (Springer, Cham, 2021), pp. 17-28. https://doi.org/10.1007/978-3-030-83643-6_2
23. J. Fort, Human Popul. Genet. Genom. **2**, 0003 (2022)
24. K. Gagal, G.R. Sarson, A. Shukurov, PLoS One **9**, e95714 (2014)
25. J.-P. Bocquet-Appel, S. Naji, M. vander Linden, J. Kozlowski, J. Arch. Sci. **39**, 531 (2012)
26. M. Porcic, T. Blagojevic, J. Pendic, S. Stefanovic, J. Arch. Sci.: Rep. **22**, 102528 (2020)
27. N. Isern, J. Fort, PLoS One **14**, e0215573 (2019)
28. J. Cobo, J. Fort, N. Isern, J. Arch. Sci. **101**, 123–130 (2019)
29. J.G. de Souza, J.A. Mateos, M. Madella, PLoS One **15**, e0232367 (2020)
30. A. Jerardino, J. Fort, N. Isern, B. Rondelli, PLoS One **9**, e113672 (2014)
31. N. Isern, J. Zilhao, J. Fort, A.J. Ammerman, Proc. Natl. Acad. Sci. U.S.A. **114**, 897 (2017)
32. J. Fort, Antiquity **77**, 520 (2003)
33. J. Fort, T.A. Kohler, M. Blake, in preparation (2022)
34. N. Barber, Cross-Cult. Res. **36**, 3 (2002)
35. E.R. Jones, G. Zarina, V. Moiseyev, E. Lightfoot, P.R. Nigst, A. Manica, R. Pinhasi, D.G. Bradley, Curr. Biol. **27**, 576–582 (2017)
36. J. Fort, T. Pujol, L.L. Cavalli-Sforza, Cambr. Archaeol. J. **14**, 53 (2004)
37. N. Isern, J. Fort, J. R. Soc. Interface **11**, 20140028 (2014)
38. J. Yin, J.S. McCaskill, Biophys. J. **61**, 1540 (1992)
39. L. You, J. Yin, J. Theor. Biol. **200**, 365 (1999)
40. J. Fort, J. Theor. Biol. **214**, 515 (2002)
41. J. Fort, V. Méndez, Phys. Rev. Lett. **89**, 178101 (2002)
42. N. Isern, J. Fort, V.L. de Rioja, Sci. Rep. **7**, 11229 (2017)

Open Access This chapter is licensed under the terms of the Creative Commons Attribution 4.0 International License (http://creativecommons.org/licenses/by/4.0/), which permits use, sharing, adaptation, distribution and reproduction in any medium or format, as long as you give appropriate credit to the original author(s) and the source, provide a link to the Creative Commons license and indicate if changes were made.

The images or other third party material in this chapter are included in the chapter's Creative Commons license, unless indicated otherwise in a credit line to the material. If material is not included in the chapter's Creative Commons license and your intended use is not permitted by statutory regulation or exceeds the permitted use, you will need to obtain permission directly from the copyright holder.